N-Glycosylation Deficiency Reduces the Activation of Protein C and Disrupts the Endothelial Barrier Integrity

Tiffany Pascreau[1,2] François Saller[1] Elsa P. Bianchini[1] Dominique Lasne[1,2] Arnaud Bruneel[3,4] Christelle Reperant[1] François Foulquier[5] Cécile V. Denis[1] Pascale De Lonlay[6] Delphine Borgel[1,2]

[1] HITh, UMR_S 1176, Institut National de la Santé et de la Recherche Médicale, Université Paris-Saclay, Le Kremlin-Bicêtre, France
[2] Laboratoire d'Hématologie, AP-HP, Hôpital Necker-Enfants malades, Paris, France
[3] Biochimie Métabolique et Cellulaire, AP-HP, Hôpital Bichat-Claude Bernard, Paris, France
[4] INSERM UMR1193, Université Paris-Saclay, Châtenay-Malabry, France
[5] Université de Lille, CNRS, UMR 8576–UGSF - Unité de Glycobiologie Structurale et Fonctionnelle, Lille, France
[6] Centre de référence des maladies héréditaires du métabolisme de l'enfant et de l'adulte - MAMEA, Filière G2M, MetabERN, Imagine Institute, AP-HP, Hôpital Necker-Enfants Maladies, University Paris-Descartes, Paris, France

Address for correspondence Delphine Borgel, PharmD, PhD, Hôpital Necker-Enfants Malades, 149 rue de Sèvres, Paris (e-mail: delphine.borgel@aphp.fr).

Thromb Haemost

Abstract

Phosphomannomutase 2 (PMM2) deficiency is the most prevalent congenital disorder of glycosylation. It is associated with coagulopathy, including protein C deficiency. Since all components of the anticoagulant and cytoprotective protein C system are glycosylated, we sought to investigate the impact of an *N*-glycosylation deficiency on this system as a whole. To this end, we developed a PMM2 knockdown model in the brain endothelial cell line hCMEC/D3. The resulting PMM2^{low} cells were less able to generate activated protein C (APC), due to lower surface expression of thrombomodulin and endothelial protein C receptor. The low protein levels were due to downregulated transcription of the corresponding genes (*THBD* and *PROCR*, respectively), which itself was related to downregulation of transcription regulators Krüppel-like factors 2 and 4 and forkhead box C2. PMM2 knockdown was also associated with impaired integrity of the endothelial cell monolayer—partly due to an alteration in the structure of VE-cadherin in adherens junctions. The expression of protease-activated receptor 1 (involved in the cytoprotective effects of APC on the endothelium) was not affected by PMM2 knockdown. Thrombin stimulation induced hyperpermeability in PMM2^{low} cells. However, pretreatment of cells with APC before thrombin simulation was still associated with a barrier-protecting effect. Taken as a whole, our results show that the partial loss of PMM2 in hCMEC/D3 cells is associated with impaired activation of protein C and a relative increase in barrier permeability.

Keywords
- protein C
- phosphomannomutase 2
- endothelial
- *N*-glycosylation

received
July 5, 2021
accepted after revision
February 2, 2022

Georg Thieme Verlag KG,
Rüdigerstraße 14,
70469 Stuttgart, Germany

DOI https://doi.org/10.1055/s-0042-1744378.
ISSN 0340-6245.

Introduction

Inherited congenital disorders of glycosylation (CDGs) are rare syndromes caused by genetic defects in the synthesis, attachment, or maturation of glycans before or after their linkage to proteins. The most prevalent CDG is phosphomannomutase 2 (PMM2) deficiency (PMM2-CDG).[1] PMM2 is a cytosolic enzyme that catalyzes the isomerization of mannose 6-phosphate to the mannose 1-phosphate required in the first steps of the *N*-glycosylation process.[2] PMM2-CDG results in neurological impairment and multivisceral dysfunction. During periods of fever, patients with PMM2-CDG can develop stroke-like episodes. Thromboses and hemorrhages have also been reported in CDG.[3–6] The hemostatic system's role in the pathophysiology of stroke-like episode has not yet been characterized, although elevated thrombin generation has been observed in patients with a history of stroke-like episode.[7] Coagulation factors—most of which are glycoproteins—are also frequently affected in CDG. The prevalence of protein C (PC) deficiency in patients with PMM2-CDG ranges from 29 to 72%.[3,5,7]

PC is part of a complex system involved in both hemostasis and the cellular response to vascular and inflammatory injury.[8] PC circulates in the plasma and is activated by thrombin on the surface of endothelial cells to give activated PC (APC). This activation involves the membrane receptors thrombomodulin (TM) and the endothelial PC receptor (EPCR). APC exerts its anticoagulant effects, thus limiting thrombin generation. APC also displays endothelial-barrier-protective properties.[8] APC's cytoprotective functions are linked to the protein's ability to cleave the first member in the protease-activated receptor family (PAR-1) pathway. However, thrombin can also activate PAR-1 and promote a distinct signaling cascade that results in opposing cellular responses. This phenomenon is referred to as biased signaling. Since APC and its receptors are *N*-glycosylated, we hypothesized that the PC system might be affected by an overall defect in *N*-glycosylation in PMM2-deficient endothelial cells. This might especially be the case in the brain, where TM and EPCR play prominent roles.[9,10]

The roles of the *N*-linked glycans on APC and its receptors have previously been investigated in site-directed mutagenesis experiments.[11–15] However, each of these studies focused on a single member of the PC system and did not address the effects of *N*-linked glycosylation on this multicomponent system as a whole. To gain insights into the functional status of the PC system in PMM2-CDG, we generated an endothelial cell line in which the expression of PMM2 was knocked down. We evaluated the PMM2-deficient endothelial cell line's ability to generate APC and to maintain an endothelial barrier function under basal and inflammatory conditions.

Methods

Antibodies and Other Reagents

Rabbit polyclonal anti-PMM2 was purchased from Proteintech (Euromedex, Souffelweyersheim, France). Mouse monoclonal anti-β-actin (clone AC-15) was purchased from Sigma (St. Quentin Fallavier, France). PE mouse anti-human CD141, PE mouse immunoglobulin G (IgG)1κ isotype control, and mouse anti-human CD144 antibody were purchased from BD Biosciences (Le Pont-de-Claix, France). Mouse monoclonal antithrombin receptor (WEDE15) was purchased from Beckman-Coulter (Immunotech, Marseille, France). Rabbit polyclonal anti-LAMP1, normal mouse IgG, and goat anti-mouse IgG1 PE were purchased from Santa Cruz (Clinisciences, Nanterre, France). Mouse monoclonal anti-EPCR (JRK 1494) was kindly provided by Charles T. Esmon (University of Oklahoma, Norman, Oklahoma, United States). Donkey anti-mouse IgG antibody Alexa fluor 647 and ProLong Gold Antifade Mountant with 4',6-diamidino-2-phenylindol (DAPI) were purchased from ThermoFisher Scientific (Illkirch, France).

Cell Culture

The human brain microvascular endothelial cell line hCMEC/D3 (first described by Weksler et al was cultured in endothelial basal medium-2 (EBM-2; Lonza, Levallois-Perret, France) supplemented with 5% fetal bovine serum (ThermoFisher Scientific), 10 mM HEPES buffer (ThermoFisher Scientific), 1% penicillin-streptomycin (ThermoFisher Scientific), 1% chemically defined lipid concentrate (ThermoFisher Scientific), 1.4 µM hydrocortisone (Sigma), 5 µg/mL ascorbic acid (Sigma), and 1 ng/mL basic fibroblast growth factor (Peprotech, Neuilly-sur-Seine, France). Cells were maintained at 37°C in 95% air and 5% CO_2 and used between passages 37 and 43.

shRNA Transfection

hCMEC/D3 cells were cultured in six-well plates at 2.5×10^5 cells/well until they reached 50% confluence. The cells were then transfected with 2 µg of a plasmid encoding an shRNA targeting *PMM2* (Santa Cruz, Clinisciences), according to the manufacturer's instructions and using GeneCellin BCC transfection reagent (Labomics, Clinisciences). As a control, hCMEC/D3 cells were transfected with plasmids encoding scrambled shRNAs (OriGene, Clinisciences). The medium was replaced 8 hours after transfection, and 2.5 µg/mL puromycin (Clinisciences) was added 48 hours later. Transfected cells were cultured for 3 weeks, and puromycin-resistant clones were then selected. The *PMM2* shRNA-treated cells will henceforth be referred to as $PMM2^{low}$ cells.

Immunoblotting Assays

Cells were washed with Dulbecco's phosphate-buffered saline (DPBS; PAN-Biotech, Dutscher, Issy-les-Moulineaux, France) and incubated at 4°C for 5 minutes with an appropriate volume of RIPA buffer (25 mM Tris-HCl, 150 mM NaCl pH 7.6, 1.5 mM EDTA, 1% NP40, 1% sodium deoxycholate, 0.1% SDS, 6.25 mM NaF, 12.5 mM β-glycerophosphate, and 1.25 mM $NaVO_3$) supplemented with a protease inhibitor cocktail (ThermoFisher Scientific). A total of 20 µg of protein was mixed with Laemmli buffer (62.5 mM Tris-HCl [pH 6.8], 2% SDS, 10% glycerol, 25 mM dithiothreitol, and 0.01% bromophenol blue). Nonreducing conditions were used to detect LAMP1. The lysates were

separated on NuPAGE 4–12% Bis-Tris gels (ThermoFisher Scientific) and transferred to a nitrocellulose membrane (Hybond ECL, GE Healthcare, Dutscher). The membranes were blocked in 50 mM Tris-HCl, 150 mM NaCl, pH 7.4 containing 0.1% Tween-20 (TBS-T buffer), incubated overnight at 4°C with primary antibodies (diluted 1:500 for PMM2, and 1:1,000 for β-actin), and incubated with peroxidase-conjugated secondary goat anti-rabbit or goat anti-mouse antibodies (1:20,000). Signals were detected using a chemiluminescent substrate (Super Signal West Pico Chemiluminescent Substrate, ThermoFisher Scientific) and imaged using a Syngene G:box iChemiXT imager (Syngene, Cambridge, United Kingdom). The signal intensities were quantified using ImageJ software (W. Rasband, National Institutes of Health) and normalized against the β-actin signal.

Quantitative Reverse Transcriptase Polymerase Chain Reaction

RNA was purified with the Nucleospin RNA Plus kit reagent (Macherey-Nagel, Hoerdt, France), according to the manufacturer's instructions. The complementary DNAs (cDNAs) were prepared from 500 ng of total RNA by using the High-Capacity cDNA Reverse Transcriptase kit from Applied Biosystems (ThermoFisher Scientific). Quantitative PCR (qPCR) reactions were performed with Master Mix Gene Expression (Applied Biosystems, ThermoFisher Scientific) or iTaq universal SybR Green Supermix (Biorad, Marne-la-Coquette, France) on a CFX96 thermocycler (Biorad). The TaqMan probes Hs03044607_g1, Hs00264920_s1 and Hs00197387_m1, Hs00360439_g1, Hs00358836_m1, and Hs00270951_s1 (Applied Biosystems) were used to quantify the messenger RNA (mRNA) levels of PMM2, THBD, PROCR, KLF2, KLF4, and FOXC2, respectively. The forward and reverse primers were respectively 5′CTCAGAAGATGCCTCCGGAT3′ and 5′GAGCACAGACACAAACAGCA3′ for human thrombin receptor, 5′GGCATCCTCACCCTGAAGTA3′ and 5′GCACACGCAGCTCATTGTAG3′ for β-actin, and 5′CAGCCTCAAGATCATCAGCA3′ and 5′TGTGGTCATGAGTCCTTCCA3′ for GAPDH.

Protein C Activation on hCMEC/D3 Cells

PC activation was previously described.[16] Confluent hCMEC/D3 cells in 48-well plates were washed with Hank's balanced salt solution (HBSS) and then incubated for 5 minutes with 0.1% bovine serum albumin in HBSS solution containing 3 mM $CaCl_2$ and 0.6 mM $MgCl_2$ before adding 0.1 µM PC (Protexel, LFB, Courtaboeuf, France). PC was activated by the addition of 10 nM human thrombin (Kordia, Asnières, France). After a 4-hour incubation at 37°C, the reaction was stopped by adding a mixture of antithrombin (Aclotine, LFB; final concentration 1.66 mg/mL) and unfractionated heparin (Héparine Choay, Sanofi-Aventis, Gentilly, France; final concentration: 1.4 IU/mL). The supernatants were transferred into a 96-well microplate, and the amidolytic activity of APC was measured using a specific peptide substrate (p-Glu-Pro-Arg-pNa, Biophen CS-2166, Hyphen Biomed, Neuville-sur-Oise, France) at a final concentration of 0.2 mM. The rate of substrate cleavage was measured with a Vmax microplate reader (SAFAS, Monaco, France). The concentration of enzyme in the reaction mixture was determined by comparison with a standard curve generated with freshly prepared recombinant human APC (Xigris, Eli Lilly, Indianapolis, Indiana, United States). A similar experiment was performed with hypoglycosylated PC (see below), rather than native PC.

Treatment of Protein C with Peptide *N*-Glycosidase F

To prepare hypoglycosylated PC, PC was treated with peptide *N*-glycosidase F (PNGase F) (New England Biolabs, Evry, France). Then 4 µg of PC was incubated with PNGase F (12,500 U/mL) under native conditions at 37°C for 6 hours. Hypoglycosylated PC was then purified by anion-exchange chromatography on a Resource Q column equilibrated with 25 mM Tris-HCl, 25 mM NaCl, pH 7.4. Hypoglycosylated PC was eluted using a linear gradient of NaCl (25–500 mM).

Flow Cytometry Analysis

Cells were washed twice with DPBS and detached with a nonenzymatic cell dissociation solution (Accumax, Sigma) before centrifugation at 250 g for 5 minutes. The cell pellets were resuspended to a concentration of 10×10^6/mL in DPBS. Next, 2×10^5 cells were incubated for 15 minutes at room temperature with primary antibodies: anti-TM (1:5), anti-EPCR (1:1,000), anti-PAR-1 (10 µg/mL), normal mouse IgG (1:5), or PE mouse IgG1κ isotype control (1:5). Fluorescence was acquired with a BD Accuri C6 cytometer (BD Biosciences) and analyzed with BD Accuri C6 software (BD Biosciences).

Fluorescence Microscopy

Cells were fixed with 4% paraformaldehyde in 1X PBS for 20 minutes at room temperature, washed with 1X PBS containing 0.05% Tween-20, and permeabilized with 0.1% Triton X-100 in 1X PBS for 5 minutes at room temperature. The fixed cells were blocked for 30 minutes at room temperature in blocking solution (1% BSA in 1X PBS). The primary anti-VE-cadherin (CD144) antibody was diluted (1:100) in blocking solution and incubated for 1 hour at room temperature. The cells were washed. The secondary Alexa Fluor 647-conjugated anti-mouse IgG antibody was diluted in 1X PBS (2 µg/mL) and incubated for 1 hour at room temperature. TRITC-conjugated phalloidin (1:4,000) (Merck Millipore, Guyancourt, France) was incubated simultaneously. After washing, the coverslips were mounted on a slide using ProLong Gold Antifade Mountant containing DAPI. Fluorescence images were visualized with a fluorescence microscope (Eclipse E600, Nikon). We used an apochromatic 60×1.40 oil differential interference contrast H60 Plan objective for image acquisition. Images were analyzed with ImageJ software.

Transendothelial Permeability Assay

hCMEC/D3 cells were seeded onto collagen-coated Transwell inserts with a 3 µm pore size (Greiner Bio-one, Les Ulis, France) and cultured for 48 hours. The culture medium was then changed, and inserts were placed in new wells containing HBSS solution. Next, a solution containing 4% BSA and 0.67 mg/mL Evans blue was added to the apical chamber. After 15 minutes, the medium from the lower chamber was sampled and its absorbance at 650 nm was measured with a spectrophotometer.

Real-Time Cell Analysis

The endothelial barrier function was assessed using the iCELLigence real-time cell analysis (RTCA) system (ACEA Biosciences, San Diego, California, United States). This impedance-based system measures transendothelial electrical resistance (the cell index [CI]) in real-time through gold microelectrodes integrated into a culture plate (E-plate L8). Cells (10^5/well) were cultured on E-plates coated with 0.1% gelatin until they reached confluence. Endothelial permeability was measured by treating confluent cells with 1 nM of thrombin after a 4 hour-incubation (or not) with 20 nM of APC. Each condition was tested in duplicate, and results were expressed as the CI after normalization against the value at baseline (i.e., prior to stimulation).

Statistical Analysis

Data were described as the mean ± standard deviation. Shapiro–Wilk tests were used for testing normality of continuous variables. A two-tailed Student *t*-test (parametric) or Mann–Whitney U-test (nonparametric) were performed for comparison of two groups. Analysis of variance (ANOVA) or Kruskal–Wallis tests (nonparametric) were used for comparison of more than two groups with Bonferroni's or Dunn's multiple comparison test, respectively, for pairwise comparisons. The threshold for statistical significance was set to $p < 0.05$. Statistical analysis was performed using Prism 8 software (GraphPad, San Diego, California, United States).

Results

APC Generation is Impaired in PMM2^{low} Cells

To investigate the impact of PMM2 deficiency on the endothelial components of the PC system, we first used RNA interference to knock down PMM2 expression in the hCMEC/D3 cell line. The PMM2^{low} cells expressed moderately low levels of PMM2 protein and mRNA (64% ± 18% and 51% ± 5% of the control values, respectively; ►**Fig. 1A, B**). This moderate decrease in PMM2 expression was enough to impair *N*-linked glycosylation, since a shift in the electrophoretic mobility of LAMP1 indicating the presence of hypoglycosylated forms was observed in PMM2^{low} cells (►**Fig. 1C**). We also found that PMM2^{low} cells were impaired in their ability to generate APC. Indeed, the activation of PC was significantly lower in PMM2^{low} cells than in control cells (16.9 ± 8.7 nM vs. 54.5 ± 14.8 nM, respectively; $p = 0.0006$) (►**Fig. 2A**). To better mimic the PMM2-CDG situation in which PC's *N*-linked glycosylation is abnormal, we also performed the experiment with PNGase-F-treated PC (i.e., PC from which the *N*-glycans had been removed). In PMM2^{low} cells, the ability to activate PC was reduced independently of PC glycosylation (►**Fig. 2B**), suggesting that the PC glycosylation would not play a major role in its activation in PMM2^{low} cells.

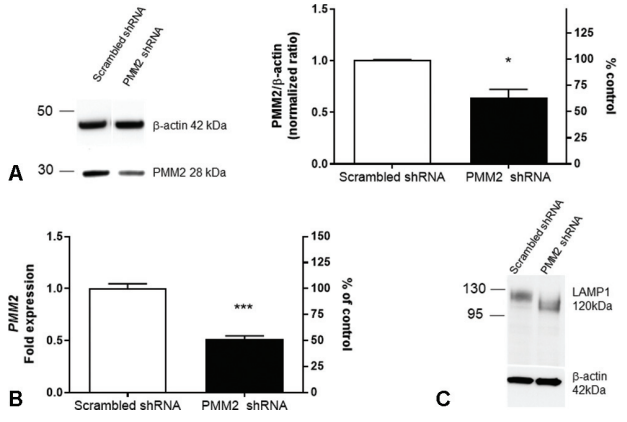

Fig. 1 Characterization of the PMM2^{low} cell line. **(A)** *Left*: A Western blot analysis of PMM2 in whole cell lysates of PMM2^{low} cells (PMM2 shRNA) and control cells (scrambled shRNA). *Right*: Protein levels of PMM2, normalized against β-actin. The results of five independent experiments are shown. Comparisons by unpaired Student's *t*-test (Welch's correction). **(B)** RT-qPCR analysis of PMM2 mRNA levels in PMM2^{low} cells and control cells. Comparisons by unpaired Student's *t*-test. **(C)** A Western blot analysis of LAMP1 normalized against β-actin in whole cell lysates of PMM2^{low} cells and control cells. $^{*}p < 0.05$; $^{***}p < 0.001$. RT-qPCR, quantitative reverse transcriptase polymerase chain reaction.

The *N*-Glycosylation Defect Reduces the Surface Expression of TM and EPCR

To account for the decrease in PC activation on the surface of PMM2^{low} cells, we used flow cytometry to assess the expression of the membrane receptors involved in this process (i.e., TM and EPCR). In PMM2^{low} cells, the levels of membrane expression of TM and EPCR were respectively 18% ± 1% ($p < 0.001$) and 71% ± 5% ($p < 0.01$) of the control values (►**Fig. 2C, F**). Hypoglycosylation may lead to an endoplasmic reticulum retention of misfolded forms of TM and EPCR prior their degradation by the ubiquitin-proteasome system.[17] To test this hypothesis, flow cytometry experiments were performed on permeabilized **(►Supplementary Fig. S1**, available in the online version**)** cells treated or not with MG132 (a proteasome inhibitor) **(►Supplementary Fig. S2**, available in the online version**)**. No rescue in the expression of TM and EPCR was seen after permeabilization and/or MG132 treatment. Similarly, the low level of surface receptors was not due to greater proteolytic cleavage of TM and EPCR, since the concentrations of the soluble forms of TM (sTM) and EPCR (sEPCR) in the culture medium were lower in PMM2^{low} cells than in control cells (respectively 2.4 ± 1 vs. 32.8 ± 4.8 ng/mL for sTM; $p < 0.001$; and 3.4 ± 0.3 vs. 6.0 ± 0.2 ng/mL for sEPCR; $p < 0.001$) **(►Fig. 2D, G**). Lastly, we found that the levels of *THBD* and *PROCR* transcripts (the genes coding for TM and EPCR, respectively) were lower in PMM2^{low} cells (respectively 18% ± 5% ($p < 0.001$) and 34% ± 2% ($p < 0.001$) of the values in control cells) (►**Fig. 2E, H**).

Since the transcription factors KLF2 and KLF4 reportedly regulate *THBD* gene expression, we used reverse transcriptase qPCRs (RT-qPCRs) to quantify KLF2 and KLF4 mRNA levels. In PMM2^{low} cells, the levels of KLF2 and KLF4 mRNA were respectively 58% ± 17% ($p = 0.0064$) and 34% ± 18% ($p = 0.0003$) of the values in control cells (►**Fig. 3A, B**). The mRNA levels of another transcription factor (FOXC2, known to regulate both *THBD* and *PROCR* gene expression) were also abnormally low in PMM2^{low} cells, albeit to a lesser extent (►**Fig. 3C**).

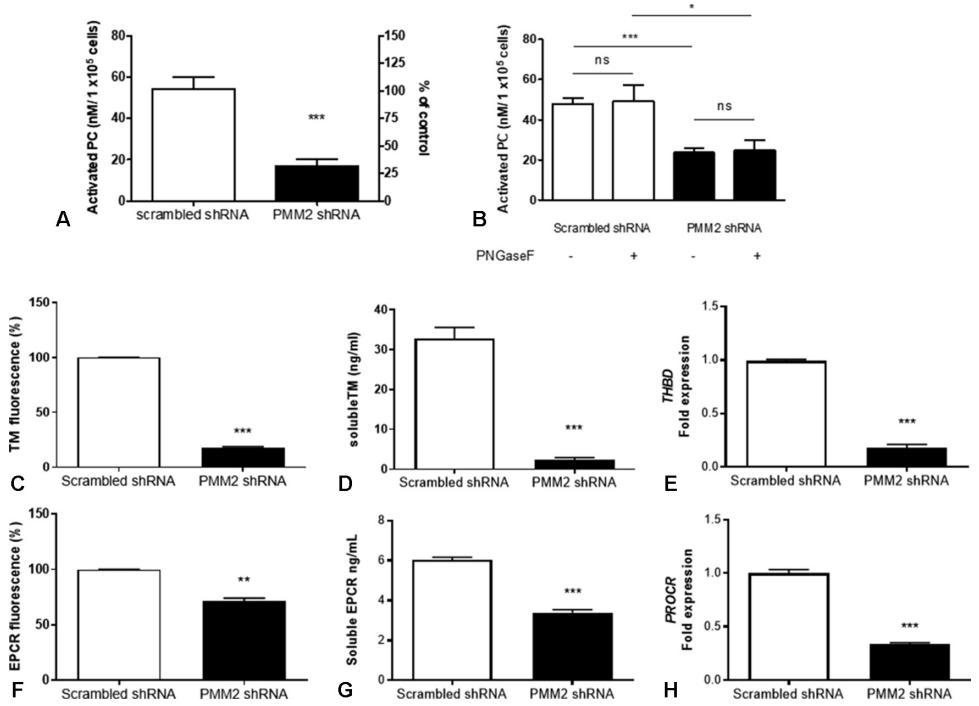

Fig. 2 Protein C activation on hCMEC/D3 cells. **(A)** After a 4-hour incubation with 0.1 µM PC and 10 nM human thrombin, the amidolytic activity of the APC generated was measured using a chromogenic substrate (S-2366). The results are expressed in nM of APC per 100,000 cells. Comparisons by Mann–Whitney U-test. **(B)** The PC activation assay was also performed with PC pretreated with PNGase F. Comparisons by analysis of variance (ANOVA). $^{*}p < 0.05$; $^{**}p < 0.01$. **(C, F)** Flow cytometry analysis of TM and EPCR. The results were expressed as mean values of fluorescence intensity expressed as a percentage relative to control cells. Comparisons by unpaired Student's *t*-test (Welch's correction). **(D, G)** Soluble form of TM and EPCR in the cell culture supernatant. Comparisons by unpaired Student's *t*-test. **(E, H)** qPCR analysis of THBD and PROCR transcripts. Comparisons by unpaired Student's *t*-test. Results are expressed as the fold change relative to β-actin and GAPDH. $^{**}p < 0.01$; $^{***}p < 0.001$. APC, activated protein C; EPCR, endothelial protein C receptor; ns, nonsignificant; PC, protein C; qPCR, quantitative polymerase chain reaction; TM, thrombomodulin.

APC's Cytoprotective Activity Is Preserved in PMM2^{low} Cells

Given that APC reportedly protects the endothelial barrier via activation of PAR-1, we investigated whether PMM2 knockdown altered APC's ability to restore the integrity of the endothelial barrier after thrombin-induced disruption.

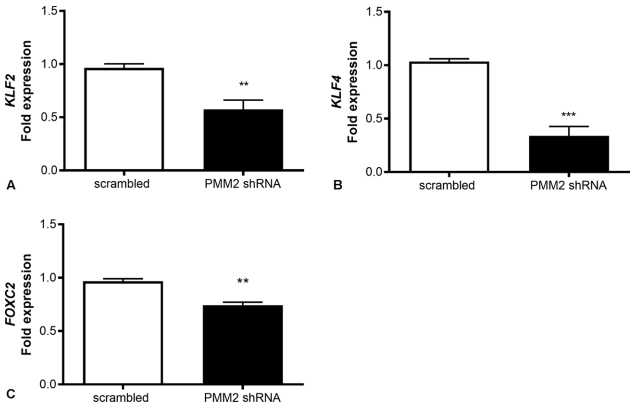

Fig. 3 KLF2, KLF4, and FOXC2 expression. KLF2, KLF4, and FOXC2 transcript levels were quantified in qPCRs. The results are expressed as the fold change relative to β-actin and GAPDH. Comparisons by unpaired Student's *t*-test. $^{**}p < 0.01$; $^{***}p < 0.001$. qPCR, quantitative polymerase chain reaction.

We first checked that the transcriptional defect observed in PMM2^{low} cells did not affect PAR-1 expression. Indeed, the membrane expression of PAR-1 in PMM2^{low} cells (as assessed using flow cytometry) was similar to that in control cells, while higher levels of PAR-1 transcripts were observed (a 1.6-fold change; $p < 0.001$) (►**Fig. 4**).

We next evaluated the integrity and permeability of PMM2^{low} and control hCMEC/D3 cells under resting conditions, using an impedance-based method.[18,19] At confluence, the maximal CI values were significantly lower for PMM2^{low} cells than for control cells (5.65 ± 1.11 vs. 9.83 ± 1.08, respectively; $p < 0.01$) (►**Fig. 5A**)—suggesting that the interendothelial junctions were impaired in PMM2^{low} cells. Since VE-cadherin is a component of the endothelial adherens junctions that are particularly important for maintaining endothelial barrier integrity (by interacting with the actin cytoskeleton[20]), we compared the cellular organization of VE-cadherin and actin cytoskeleton in PMM2^{low} versus control cells. Control cells exhibited the classical cobblestone-like morphology; the majority of the actin filaments were localized at the cell periphery and lay parallel to the cell–cell junctions. VE-cadherin formed a line at the cell–cell junctions, with occasional gaps (►**Fig. 5B**). In contrast, actin filaments in PMM2^{low} cells were found to be scattered. Furthermore, the VE-cadherin was distributed discontinuously at the cell–cell junctions. This loss of barrier integrity

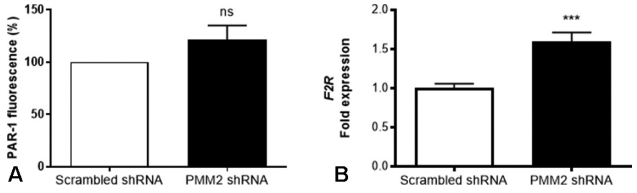

Fig. 4 PAR-1 expression. **(A)** A flow cytometry analysis of PAR-1 membrane expression. The results are expressed as mean values of fluorescence intensity expressed as a percentage relative to control cells. Comparisons by unpaired Student's *t*-test (Welch's correction). **(B)** F2R transcript levels were quantified in qPCRs. The results are expressed as the fold change relative to β-actin and GAPDH. Comparisons by unpaired Student's *t*-test; $^{***}p < 0.001$. qPCR, quantitative polymerase chain reaction.

was also confirmed in an Evans blue assay. Indeed, the transendothelial passage of an Evans blue–albumin conjugate was significantly greater through PMM2^{low} cell monolayers than through control monolayers (absorbance at 650 nm: 0.87 ± 0.15 and 0.22 ± 0.12 for PMM2^{low} and control cells, respectively, $p < 0.001$) (►**Fig. 5C**). Taken as a whole, these observations evidenced an impairment of the endothelial barrier function in PMM2^{low} cells under basal conditions.

Lastly, we used a similar cell impedance-based permeability assay to investigate the endothelial response to thrombin stimulation. In control hCMEC/D3 cells, the hyperpermeability induced by thrombin resulted in a rapid, acute decrease in the normalized CI (NCI), followed by a recovery to initial values in less than 2 hours (►**Fig. 6A**). In PMM2^{low} cells, thrombin induced a much greater maximum decrease in NCI (0.39 ± 0.12, vs. 0.93 ± 0.12 in control cells; $p < 0.01$) (►**Fig. 6B**). Thrombin's ability to disrupt the endothelial barrier (quantified by the total area under the curve) was also greater in PMM2^{low} cells than in control cells (0.19 ± 0.08 vs. 7.91 ± 0.04 NCI/hour, respectively; $p < 0.01$) (►**Fig. 6C**).

Considering the APC's PAR-1-mediated role in endothelial barrier protection, we next investigated the endothelial response to thrombin stimulation after a 4 hour-incubation with APC. Preincubation with APC cells did not prevent the decrease in CI in PMM2^{low} cells but did accelerate the NCI's return to baseline; a 50% recovery was obtained after 3.74 ± 1.37 versus 6.97 ± 0.86 hours in the presence and absence of APC, respectively ($p < 0.01$) (►**Fig. 6D**).

Discussion

To investigate the role of *N*-linked glycosylation within the PC system, we developed a brain endothelial cell line that was knocked down for PMM2. This knockdown resulted in a moderate decrease in both protein and mRNA levels of PMM2. It is likely that cells with greater decreases would not be viable. This hypothesis is supported by the fact that

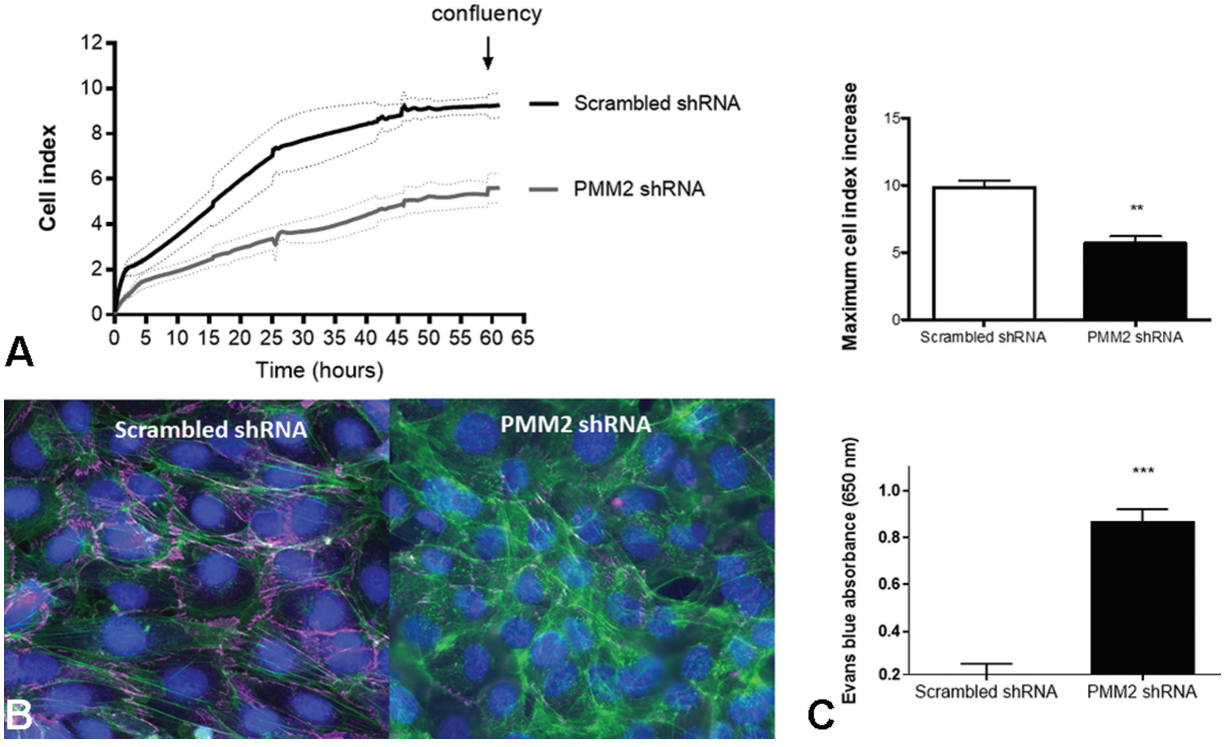

Fig. 5 Endothelial barrier integrity in the basal state. **(A)** *Left*: An RTCA during the adhesion and proliferation steps, until the cells reached confluence. The results of four independent experiments are shown. The CI was expressed as the mean (solid line) ± SD (dotted line). *Right*: The maximum increase in the CI measured during the initial adhesion and proliferation. Comparisons by unpaired Student's *t*-test. **(B)** Immunofluorescence staining. Distribution of VE-cadherin (purple) and F-actin (green). Blue, DAPI staining of nuclei. **(C)** The Evans blue permeability assay in PMM2^{low} cells, relative to control cells. Absorbance at 650 nm was measured 15 minutes after incubation with a 4% BSA Evans blue solution. Comparisons by unpaired Student's *t*-test. $^{**}p < 0.01$; $^{***}p < 0.001$. CI, cell index; RTCA, real-time cell analysis; SD, standard deviation.

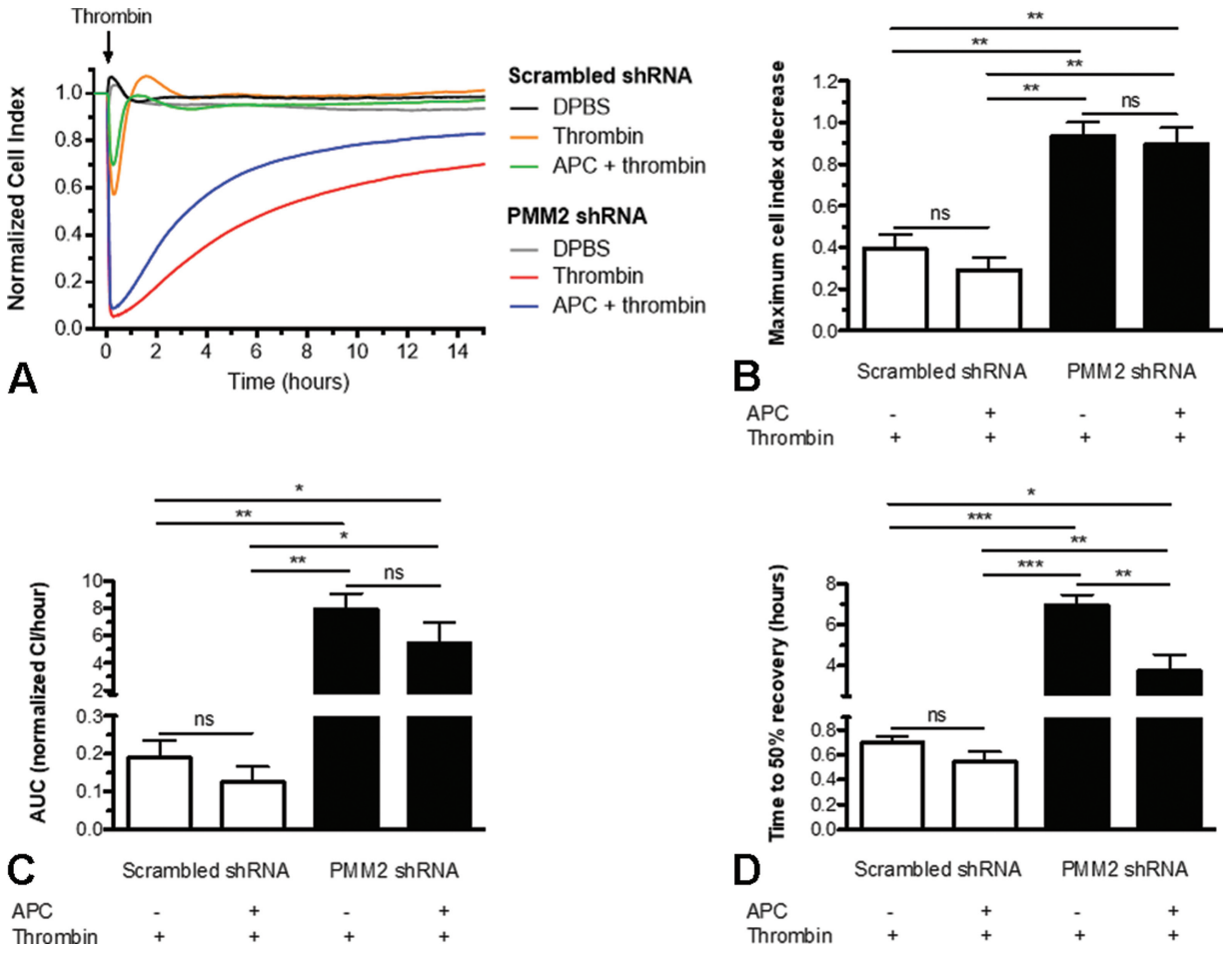

Fig. 6 Real-time cell analysis following thrombin stimulation. **(A)** An RTCA of cells incubated with 20 nM APC for 4 hours prior to thrombin stimulation (1 nM). The curves show the mean CI from a single experiment. **(B)** The maximum decrease in the CI in response to stimulation with 1 nM thrombin, expressed as the difference between untreated cells and stimulated cells. The plots are representative of three independent experiments. **(C, D)** Recovery to the baseline CI in cells incubated with 20 nM APC prior to thrombin stimulation (1 nM), expressed as the area under the curve (AUC) **(C)** and the time to 50% recovery **(D)**. The AUC was calculated as the difference between untreated cells and stimulated cells. The time to 50% recovery was the time required to recover 50% of the baseline CI. The results of three independent experiments are shown. Comparisons by analysis of variance (ANOVA). $^{*}p < 0.05$; $^{**}p < 0.01$; $^{***}p < 0.001$. APC, activated protein C; CI, cell index; ns, nonsignificant; RTCA, real-time cell analysis.

the complete loss of PMM2 in mice is embryonic-lethal before 5.5 days of development.[21] A transient transfection model of endothelial cell knockdown for PMM2 has already been developed with human umbilical vein endothelial cells[22]; the protein level of PMM2 was 70% lower but the PC system was not investigated. In the present study, we used the hCMEC/D3 cell line (derived from brain microvessels) to generate a stable knockdown of PMM2. Even though we only obtained an approximately twofold relative decrease in PMM2 expression, a major impact on *N*-linked glycosylation was evidenced by LAMP1's abnormal glycosylation profile.

All the protein components of the PC system harbor *N*-glycans that might have functional importance. We chose to investigate the anticoagulant and cytoprotective properties of the PC system in PMM2^{low} endothelial cells. First, we observed that PMM2 knockdown was associated with significantly lower APC generation, due to lower expression of the two receptors (TM and EPCR) involved in PC activation. TM is constitutively expressed on endothelial cells. It contributes to the endothelium's anticoagulant properties and thus helps prevent thrombosis. Indeed, endothelial cell-specific knockout of TM in mice leads to excessive activation of coagulation and thus fatal, massive thrombosis.[23] It remains to be seen whether the strong decrease in TM expression induced by PMM2 knockdown leads to a prothrombotic phenotype; this question fell outside the scope of our study.

Since PC is also hypoglycosylated in patients with PMM2-CDG,[24] we treated PC with PNGase F prior to the measurement of APC generation in PMM2^{low} cells. The rate of PC activation was similar with hypoglycosylated and fully glycosylated forms of PC. Previous directed mutagenesis studies showed that the rate of PC activation was elevated in the absence of *N*-linked glycosylation at Asn313.[15] This discrepancy might be explained by the introduction of the amino acid mutation rather than the loss of the glycan chain.

Interestingly, PAR-1 expression (unlike TM and EPCR expression) was not affected by PMM2 silencing—suggesting that the transcriptional machinery in our model was not fully impacted. Moreover, we did not evidence elevated degradation of potentially misfolded hypoglycosylated receptors by

the ubiquitin/proteasome system. This finding suggests that TM and EPCR downregulation might be due to the regulation of *THBD* and *PROCR* transcription. We therefore decided to explore transcription factors such as Kruppel-like factors (KLFs).[10,25] In particular, KLF2 and KLF4 are known to regulate *THBD* gene expression,[26,27(p2)] and Sangwung et al[28] showed that the endothelium-specific deletion of *Klf2* and *Klf4* in mice resulted in the near-complete loss of TM expression. Interestingly, we observed lower KLF2 and KLF4 expression in PMM2^{low} cells (relative to controls), which might account for the lower TM expression. In contrast, KLF2 and KLF4 were not involved in the regulation of *EPCR* expression in a mouse model of a cerebral cavernous malformation.[10] However, it was recently reported that the genetic knockout of a transcription factor (*FOXC2*) was associated with lower TM and EPCR expression in the perivalvular endothelium and thereby contributed to loss of the antithrombotic phenotype in mice.[29] The expression level of *FOXC2* (which might be involved in *PROCR* and *THBD* downregulation) was low in our PMM2^{low} cells.

Besides being an anticoagulant, APC also protects endothelial cells through biased PAR-1 signaling.[30] Since PAR-1 was expressed normally in the PMM2^{low} cells, we investigated the receptor's activation by thrombin and APC. As already reported in hCMEC/D3 cells,[31] we first confirmed that thrombin activates PAR-1 and leads to barrier-disruptive and proinflammatory responses. Using RTCA, we showed that thrombin induced greater permeability in PMM2^{low} cells than in control cells. This may be related to the fact that biased signaling is regulated by the *N*-linked glycan chains in the second extracellular loop of PAR-1. Indeed, it has been reported that removal of PAR-1's *N*-linked glycosylation on extracellular loop 2 reduced Rho-A-mediated stress fiber formation and enhanced cell proliferation in response to thrombin stimulation.[13,14] The increase in endothelial permeability in response to thrombin has been attributed to the disassembly and disappearance of junctional proteins at cell-to-cell contacts.[32] hCMEC/D3 cells contain junction-associated Ig-like proteins (such as PECAM-1 and JAM-A), adherens junction and tight junction structural proteins (such as VE-cadherin, claudin-3,-5, and occludin).[33] All these glycoproteins are likely to be affected by the loss of *N*-linked glycosylation,[34,35] and the resulting changes might contribute to the hyperpermeability observed in PMM2^{low} cells. In line with this hypothesis, the data from transendothelial permeability assays, RTCAs, and immunofluorescence staining of endothelial cells suggested that PMM2 knockdown reduced the integrity of endothelial cell monolayers. This reduction might be due in part to an alteration in the structure of the VE-cadherin-based adherens junction. Indeed, VE-cadherin bears sialylated *N*-glycans that are involved in the protein's function in the adherens junction.[36] An examination of embryonic PMM2$^{R137H/F118L}$ mice showed extensive degradation of multiple organs and massive hemorrhaging within the extraembryonic-supporting structures—leading to embryonic lethality.[37] Moreover, some patients with PMM2-CDG are susceptible to fluid extravasation,[38] edema, and hydrops fetalis.[39,40] The endothelial dysfunction observed in our model might thus be involved in this phenotype.

Given that PAR-1 also mediates APC's endothelial-barrier-protecting functions, we incubated PMM2^{low} cells with APC prior to thrombin stimulation. Interestingly, the 50% recovery of CI under these experimental conditions was achieved significantly more quickly after pretreatment with APC. Our results suggest that despite the lower level of EPCR expression in PMM2^{low} cells, APC can still exert its barrier-stabilizing effect. Since we know that EPCR is required for APC's cytoprotective effects,[30] it appears that residual expression of EPCR at the PMM2^{low} cell membrane is enough to enable its activity as a cofactor with APC. Overall, our results show that the almost complete loss of TM led a significant impairment in APC generation (since TM has an essential role in PC activation), whereas the partial loss of EPCR does not abrogate APC's cytoprotective effects (since EPCR acts as a coreceptor for PAR-1). Experiments performed on endothelial cells cultured under static conditions do not reflect the physiological environment of the vascular system, in particular the shear stress conditions. The same experiments could be repeated under flow and would provide additional information. In summary, our results showed that PMM2 knockdown induces lower TM and EPCR expression. This relative decrease is mediated in part by lower expression of the transcription factors KLF2/KLF4 and FOXC2. PMM2 knockdown is also associated with (1) significantly weaker APC generation, which potentially endows the endothelium with a procoagulant phenotype, and (2) an impairment of endothelial barrier integrity—a proxy for blood–brain barrier integrity. Although thrombin induced greater hyperpermeability in PMM2^{low} cells than in control cells, APC still exerted its barrier-stabilizing effect. Overall, our results provide a better understanding of *N*-glycosylation's role in the PC system and in the endothelial barrier.

What is known about this topic?

- Phosphomannomutase 2 (PMM2) deficiency is the most frequent type of congenital disorders of glycosylation. Congenital disorders of glycosylation are often associated with protein C deficiency.
- The protein C system has anticoagulant activities but also cytoprotective effects on endothelium. However, the impact of glycosylation defect on the protein C system has never been studied in congenital disorder of glycosylation.

What does this paper add?

- This is the first description of an endothelial model (hCMECD3) knockdown for PMM2 in which we have evidenced a reduction in the activation of the protein C. PMM2 deficiency also disrupts the endothelial barrier integrity and pretreatment of cells with activated protein C remains associated with a barrier-protecting effect.
- Our results provide a better understanding of *N*-glycosylation's role in the protein C system and in the endothelial barrier.

Author Contributions

T.P. performed the research, analyzed data, and wrote the manuscript; F.S. analyzed data and wrote the manuscript; E.P.B., D.L., A.B., C.V.D., and P.D.L. wrote the manuscript; F. F. contributed for reagents; C.R. performed research and analyzed data; D.B. designed the research, analyzed data, and wrote the manuscript; all authors read and approved the final version of the manuscript.

Funding

The study was funded by ERA-NET cofounding (Reference 643578) and Fondation pour la Recherche Médicale (DEA20140731350).

Conflict of Interest

None declared.

Acknowledgments

The hCMEC/D3 cell line was kindly provided by Pierre-Olivier Couraud (Cochin institute). This work was funded in part by the European Union's Horizon 2020 research and innovation program (ERA-NET cofounding, reference 643578), INSERM, Université Paris-Saclay, and the Fondation pour la Recherche Médicale (fellowship DEA20140731350 to T.P.).

References

1 Péanne R, de Lonlay P, Foulquier F, et al. Congenital disorders of glycosylation (CDG): quo vadis? Eur J Med Genet 2018;61(11): 643–663
2 Jaeken J, Péanne R. What is new in CDG? J Inherit Metab Dis 2017; 40(04):569–586
3 Schiff M, Roda C, Monin M-L, et al. Clinical, laboratory and molecular findings and long-term follow-up data in 96 French patients with PMM2-CDG (phosphomannomutase 2-congenital disorder of glycosylation) and review of the literature. J Med Genet 2017;54(12):843–851
4 Arnoux JB, Boddaert N, Valayannopoulos V, et al. Risk assessment of acute vascular events in congenital disorder of glycosylation type Ia. Mol Genet Metab 2008;93(04):444–449
5 Linssen M, Mohamed M, Wevers RA, Lefeber DJ, Morava E. Thrombotic complications in patients with PMM2-CDG. Mol Genet Metab 2013;109(01):107–111
6 Tamminga RYJ, Lefeber DJ, Kamps WA, van Spronsen FJ. Recurrent thrombo-embolism in a child with a congenital disorder of glycosylation (CDG) type Ib and treatment with mannose. Pediatr Hematol Oncol 2008;25(08):762–768
7 Pascreau T, de la Morena-Barrio ME, Lasne D, et al. Elevated thrombin generation in patients with congenital disorder of glycosylation and combined coagulation factor deficiencies. J Thromb Haemost 2019;17(11):1798–1807
8 Mosnier LO, Zlokovic BV, Griffin JH. The cytoprotective protein C pathway. Blood 2007;109(08):3161–3172
9 Griffin JH, Fernández JA, Liu D, Cheng T, Guo H, Zlokovic BV. Activated protein C and ischemic stroke. Crit Care Med 2004;32(5, Suppl)S247–S253
10 Lopez-Ramirez MA, Pham A, Girard R, et al. Cerebral cavernous malformations form an anticoagulant vascular domain in humans and mice. Blood 2019;133(03):193–204
11 Parkinson JF, Vlahos CJ, Yan SCB, Bang NU. Recombinant human thrombomodulin. Regulation of cofactor activity and anticoagulant function by a glycosaminoglycan side chain. Biochem J 1992; 283(Pt 1):151–157
12 Liaw PCY, Mather T, Oganesyan N, Ferrell GL, Esmon CT. Identification of the protein C/activated protein C binding sites on the endothelial cell protein C receptor. Implications for a novel mode of ligand recognition by a major histocompatibility complex class 1-type receptor. J Biol Chem 2001;276(11):8364–8370
13 Soto AG, Smith TH, Chen B, et al. N-linked glycosylation of protease-activated receptor-1 at extracellular loop 2 regulates G-protein signaling bias. Proc Natl Acad Sci U S A 2015;112(27): E3600–E3608
14 Soto AG, Trejo J. N-linked glycosylation of protease-activated receptor-1 second extracellular loop: a critical determinant for ligand-induced receptor activation and internalization. J Biol Chem 2010;285(24):18781–18793
15 Grinnell BW, Walls JD, Gerlitz B. Glycosylation of human protein C affects its secretion, processing, functional activities, and activation by thrombin. J Biol Chem 1991;266(15):9778–9785
16 Stearns-Kurosawa DJ, Kurosawa S, Mollica JS, Ferrell GL, Esmon CT. The endothelial cell protein C receptor augments protein C activation by the thrombin-thrombomodulin complex. Proc Natl Acad Sci U S A 1996;93(19):10212–10216
17 Hwang J, Qi L. Quality control in the endoplasmic reticulum: crosstalk between ERAD and UPR pathways. Trends Biochem Sci 2018;43(08):593–605
18 Crone C, Christensen O. Electrical resistance of a capillary endothelium. J Gen Physiol 1981;77(04):349–371
19 Srinivasan B, Kolli AR, Esch MB, Abaci HE, Shuler ML, Hickman JJ. TEER measurement techniques for in vitro barrier model systems. J Lab Autom 2015;20(02):107–126
20 Giannotta M, Trani M, Dejana E. VE-cadherin and endothelial adherens junctions: active guardians of vascular integrity. Dev Cell 2013;26(05):441–454
21 Thiel C, Lübke T, Matthijs G, von Figura K, Körner C. Targeted disruption of the mouse phosphomannomutase 2 gene causes early embryonic lethality. Mol Cell Biol 2006;26(15):5615–5620
22 He P, Srikrishna G, Freeze HH. N-glycosylation deficiency reduces ICAM-1 induction and impairs inflammatory response. Glycobiology 2014;24(04):392–398
23 Isermann B, Hendrickson SB, Zogg M, et al. Endothelium-specific loss of murine thrombomodulin disrupts the protein C anticoagulant pathway and causes juvenile-onset thrombosis. J Clin Invest 2001;108(04):537–546
24 Stibler H, Holzbach U, Tengborn L, Kristiansson B. Complex functional and structural coagulation abnormalities in the carbohydrate-deficient glycoprotein syndrome type I. Blood Coagul Fibrinolysis 1996;7(02):118–126
25 Pathak R, Shao L, Chafekar SM, et al. IKKβ regulates endothelial thrombomodulin in a Klf2-dependent manner. J Thromb Haemost 2014;12(09):1533–1544
26 Villarreal G Jr, Zhang Y, Larman HB, Gracia-Sancho J, Koo A, García-Cardeña G. Defining the regulation of KLF4 expression and its downstream transcriptional targets in vascular endothelial cells. Biochem Biophys Res Commun 2010;391(01):984–989
27 Lin Z, Kumar A, SenBanerjee S, et al. Kruppel-like factor 2 (KLF2) regulates endothelial thrombotic function. Circ Res 2005;96(05): e48–e57
28 Sangwung P, Zhou G, Nayak L, et al. KLF2 and KLF4 control endothelial identity and vascular integrity. JCI Insight 2017;2 (04):e91700
29 Welsh JD, Hoofnagle MH, Bamezai S, et al. Hemodynamic regulation of perivalvular endothelial gene expression prevents deep venous thrombosis. J Clin Invest 2019;129(12):5489–5500
30 Griffin JH, Zlokovic BV, Mosnier LO. Activated protein C: biased for translation. Blood 2015;125(19):2898–2907
31 Alabanza LM, Bynoe MS. Thrombin induces an inflammatory phenotype in a human brain endothelial cell line. J Neuroimmunol 2012;245(1–2):48–55
32 Komarova YA, Mehta D, Malik AB. Dual regulation of endothelial junctional permeability. Sci STKE 2007;2007(412):re8

33 Weksler BB, Subileau EA, Perrière N, et al. Blood-brain barrier-specific properties of a human adult brain endothelial cell line. FASEB J 2005;19(13):1872–1874
34 Scott DW, Tolbert CE, Graham DM, Wittchen E, Bear JE, Burridge K. N-glycosylation controls the function of junctional adhesion molecule-A. Mol Biol Cell 2015;26(18):3205–3214
35 Lertkiatmongkol P, Paddock C, Newman DK, Zhu J, Thomas MJ, Newman PJ. The role of sialylated glycans in human platelet endothelial cell adhesion molecule 1 (PECAM-1)-mediated trans homophilic interactions and endothelial cell barrier function. J Biol Chem 2016;291(50):26216–26225
36 Geyer H, Geyer R, Odenthal-Schnittler M, Schnittler H-J. Characterization of human vascular endothelial cadherin glycans. Glycobiology 1999;9(09):915–925
37 Schneider A, Thiel C, Rindermann J, et al. Successful prenatal mannose treatment for congenital disorder of glycosylation-Ia in mice. Nat Med 2011;18(01):71–73
38 Truin G, Guillard M, Lefeber DJ, et al. Pericardial and abdominal fluid accumulation in congenital disorder of glycosylation type Ia. Mol Genet Metab 2008;94(04):481–484
39 Makhamreh MM, Cottingham N, Ferreira CR, Berger S, Al-Kouatly HB. Nonimmune hydrops fetalis and congenital disorders of glycosylation: a systematic literature review. J Inherit Metab Dis 2020;43(02):223–233
40 Léticée N, Bessières-Grattagliano B, Dupré T, et al. Should PMM2-deficiency (CDG Ia) be searched in every case of unexplained hydrops fetalis? Mol Genet Metab 2010;101(2-3):253–257

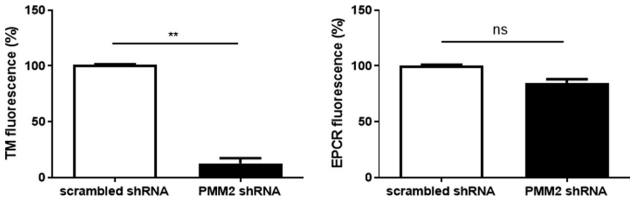

Supplementary Fig. S1 TM and EPCR expression on permeabilized cells. Cells were permeabilized using PBS1X-Triton 0.1% prior to a flow cytometry analysis of TM and EPCR membrane expression. The results are expressed as a percentage of the fluorescence observed in control cells. Comparisons by unpaired Student's *t*-test. ns: nonsignificant, $^{**}p < 0.01$. EPCR, endothelial protein C receptor; TM, thrombomodulin.

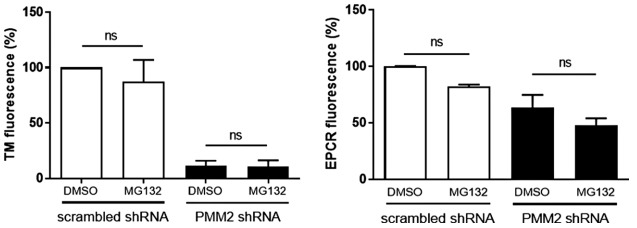

Supplementary Fig. S2 TM and EPCR expression after proteasome inhibition. Cells were pretreated (or not) with 20 µM MG132 for 19 hours, prior to a flow cytometry analysis of TM and EPCR membrane expression. The results are expressed as a percentage of the fluorescence observed in control cells. Comparisons by unpaired Student's *t*-test. EPCR, endothelial protein C receptor; ns, nonsignificant; TM, thrombomodulin.

